Indian Journal of Engineering & Materials Sciences
Vol. 31, April 2024, pp. 284-296
DOI: 10.56042/ijems.v31i2.4238

Chemiresistive room temperature methanol sensing by chemically synthesized CdSe/ZnO nanocomposites

Pallabi Boro, Pratyush Phukan, Sultana Rijuwana Haque & Suparna Bhattacharjee*
Department of Applied Sciences, Gauhati University, Guwahati 781 014, India

Received: 20 July 2023; Accepted: 21 January 2024

In this work, a chemical reaction technique has been employed to synthesize CdSe nanoparticles and CdSe/ZnO nano-composites. The synthesized samples have been characterized by different characterization methods. Study of selectivity of the synthesized samples towards different gases such as ammonia, acetone, methanol, formaldehyde and ethanol has been carried out. The synthesized CdSe and CdSe/ZnO samples have been found to be more selective towards methanol gas. As such, gas sensing ability of both CdSe and CdSe/ZnO samples towards methanol gas has been investigated. It is observed that, CdSe/ZnO nano composites have been more sensitive towards methanol gas as compared to CdSe nanoparticles.

Keywords: Selectivity, Response time, Recovery time, Selectivity, Sensitivity.

1 Introduction

Gas sensors are the unique chemical sensors, which show changes in one or more physical properties, such as resistance, conductance, absorbance, etc. upon sensing a target gas[1]. Metal oxides find widespread use as chemiresistive materials for gas sensing applications. This happens due to their adjustable electrical properties, reduced particle size, improved surface morphologies, good structural stability etc[2]. Optoelectronics, piezoelectrics, solar cells, spintronics, gas sensors etc. are some important areas where metal oxides find applications[3]. Moreover, use of dopants and variation of the working temperature and humidity under sensing conditions can be utilized to increase the sensitivity of metal oxide-based gas sensors. It is possible to analyse the electrical characteristics of the sensing material by using a mechanism of electron transfer that occurs during the reactions between the surface and the adsorbed gas molecules[3]. Temperature affects the adsorption capacity of gas sensors, and when voltage or current changes, the resistance values of the sensor can be recorded to determine the response value[4].

The interaction which occurs between the adsorbed oxygen and the analyte species is termed as reponse of the sensor. Sensitivity of a gas sensor depends on the distribution of charges on its surface and also on the diffusion of gas molecules. The morphology and amount of active sites present for interaction also affects the sensitivity[2] . At present, the synthesis of more innovative and diversified nanostructured materials that are capable of functioning as smart sensors in a variety of application areas is receiving immense attention from researchers. Semi conducting materials are most preferred ones for use as sensors in the detection of toxic and harmful gases, due to their large surface area, desirable size, physical and chemical properties, ease of synthesis etc. Sensing devices are nowadays developed as an imperious need to control the air quality. The necessity of the present times is to use cost effective material for this purpose and this is where metal oxide based gas sensors are reliable materials due to their excellent response for a broad range of gases[5]. The primary application of gas sensors is the detection of hazardous and explosive gas leaks, which can result in serious accidents, health risks, etc. These days, gas sensors are widely used in practically every industry.

Among II-VI semiconductor nanoparticles, colloidal CdSe nanoparticles have received the greatest attention due to their easily adjustable emission, which can be tuned to cover a broad wavelength range as their size decreases[6]. It has a direct band gap of 1.74 eV, is transparent to visible light, is non-toxic, has good chemical stability, and many other unique qualities[7]. Due to these unique characteristics, CdSe nanoparticles are becoming a valuable material for a wide range of applications, including sensors, field effect transistors (FET), photodetectors, and solar cells[8]. It is possible to

*Corresponding author (E-mail: suparnabhattacharjee3@gmail.com)

grow CdSe in cubic, hexagonal, or mixed (hexagonal-cubic) structures[9]. CdSe nanoparticles have been created by researchers employing a variety of physical and chemical techniques. Group II–VI semiconductor material ZnO is similarly adaptable and has numerous significant characteristics, including a broad and direct band gap of 3.37 eV, non-toxicity, strong chemical stability, antibacterial qualities, and many more[10]. Because of its wide band gap, ZnO is therefore used in many different fields and is regarded as a significant shell-forming material. Group II–VI semiconductor /semiconductor core/shell nano materials are CdSe/ ZnO nano composites. The literature contains very few reports on the synthesis of CdSe/ZnO nano composites. In 2011, the aqueous synthesis of CdSe/ZnO nanoparticles was done by B. P. Rakgalakane *et al*.[11], who used a Cd salt and $NaBH_4$ with Se to produce CdSe in the presence of thioglycerol as a stabiliser. The formation of CdSe/ZnO nanoparticles was confirmed by the characterization results. The study of photoconductivity and visible light activated room temperature gas sensing properties of nanocrystalline ZnO thick films sensitised with colloidal CdSe quantum dots was reported by A.S. Chizhov *et al*. in 2014[12]. Their findings showed that the produced CdSe/ZnO nanocomposites can be used for NO2 detection at room temperature without the need for thermal heating when exposed to visible light. Shan *et al*. carried out a study in 2005 to investigate the structure and characteristics of CdSe nanocrystals capped ZnO layer with the aim of phase transfer from hexane to ethanol solution[13]. Suo *et al*., in 2010 fabricated polynano composite thin film reinforced with CdSe-ZnS quantum dots by drop casting method and studied their optical properties[14]. The SILAR controlled CdSe nanoparticles sensitized ZnO nanorods photoanode at room temperature (27°C) for use as a solar cell was investigated by Nikam *et al*.[15] in 2018. They used different electrolytes and varied the SILAR cycles for CdSe in order to record the photovoltaic performance of the cells. In 2019, Wang *et al*. investigated conductive polymer nanolayer modified one-dimensional ZnO/CdSe photoanode with improved photochemical properties[16]. They did this by using the in-situ ions exchange method. The ZnO/CdSe-diethlenetria minenano composite was synthesised by Li *et al*. in 2020 as a step scheme for the photocatalytic evolution of hydrogen[17].

Different types of gas sensors with distinct operating principles have been developed and studied on occasion. These include resistive-based gas sensors, quartz crystal microbalance gas sensors, electrochemical gas sensors, optical gas sensors, gas chromic gas sensors, catalytic gas sensors, thermal-conductivity gas sensors, and surface acoustic wave gas sensors[18]. In this paper we report study on the gas sensing properties of CdSe and CdSe/ZnO core/shell nano composites towards methanol gas. CdSe/ZnO is a metal oxide based composite gas sensor. Various binary, ternary and more complex metal oxides can be used to study the sensor behaviour of nanomaterials towards various gases[19]. In general, either n- or p-type metal oxide semiconductors can be used for gas sensing[20]. According to Kim and Lee[21], SnO_2, ZnO, TiO_2, WO_3, In_2O_3, and Fe_2O_3 (with n-type conductivity) are the most common metal oxides used in gas sensors. This is mainly due to the high mobility of electrons in n-type metal oxides.

Methanol plays a vital role in all forms of life as it is widely used as one of the most important industrial raw materials in the chemical industry, refrigeration system, fertilizer production, live breeding and food processing. Methanol is a common feed stock for several important chemicals and an energy carrier for a clean and sustainable future[22]. It is also a very useful organic solvent with widespread applications in the manufacturing industries of colours, dyes, drugs, perfumes, formaldehyde, etc. Methanol is toxic and fatal to human beings even in modest concentrations. The wide range of applications of methanol, it's toxicity, and the desirability to be able to fine tune its synthesis under demanding conditions strongly suggest the need of development of reliable and selective methanol detection device[23]. Compared with the various traditional analytical systems, gas sensors have been acknowledged as simple and inexpensive tools for detection and quantification of toxic, harmful, flammable, and explosive gases. It is well known that gas sensors are the devices composed of active sensing materials coupled with a signal transducer. Therefore, the selection and development of a potential sensing material play an important role in designing high performance gas sensors. In the past few decades, metal oxide semiconductor based gas sensors have been extensively investigated for various daily and industrial applications due to their outstanding sensing performance, even in harsh environments[24]. In 2017, M Ando *et al*.[25] studied the

sensitivity of CdSe based quantum dots such as CdSe/ZnS, CdSeTe/ZnO etc. towards amine (primary, secondary and tertiary). They found that sensitivity of CdSe quantum dots were not affected by O_2, N_2, Ar, CO_2, or H_2. In the year 2019 J. Van Den Broak *et al*. designed a methanol detector on the basis of the concept of separation-column sensor. They found that this sensor can be used in breath analysisor in air quality monitoring[26]. In 2019 A. Chizhov *et al*.[27] studied the gas sensor properties of hybrid material based on the ZnO nanoparticles where photoexcited electron hole pairs are different between the core and the shells. They considered two types of core/shell materials. For type I core/shell nanomaterials (CdSe/CdS) they found that the sensor activity increases towards the NO_2 gas. They found that sensitivity increases due to the photogenerated holes inside the CdSe core and the passivation of CdSe core defect states. Also they studied the sensitivity of Type II Nanoparticles such as CdS/ZnSe towards NO_2 gas. Then they compared the sensitivity results with the ZnO/CdSe Nanoparticles and ZnO(CdSe/CdS) nanoparticles. They observed that the light activated sensor sensitivity increases towards NO_2.There are many researchers who designed methanol sensors. For example in 2021, M.M Abdulah *et al*.[28] detected methanol using iron oxide (α-Fe_2O_3) doped CdSe nanoparticle by the electrochemical technique. They studied the sensitivity of as synthesized α-Fe_2O_3) doped CdSe nanoparticle in the wide linear range (0.2-800mM) with a very low detection limit of 0.041mM while the promising sensitivity was obtained in the lower range of (0.2-48mM). B. Wu *et al*. in the year 2015, synthesized, ZnO/CdSe hetero-structure core/shell Nanoparticles and studied their gas sensing properties towards ethanol at temperature 160° C. They reported that in the dark or under visible light illumination 20-fold or 3-fold better gas sensor activity can be exhibited compared to bare CdSe Nanoparticles[29]. Using a chemoresistive gas sensor (Pd-doped SnO2 nanoparticles) in 2019, J.V. Broek *et al*.[30] detected methanol gas over the ethanol gas. Without affecting ethanol levels (up to 62,000 ppm), methanol was measured in 2 minutes in the range of 1 to 1000 ppm. They found that there are emerging uses for the methanol sensor, like monitoring air quality and breadth analysis.

In our work we have designed a methanol gas sensor using CdSe and CdSe/ZnO nanoparticles as the active layer. The designed system is of low cost and simple in operation. As methanol is a very hazardous gas which can increase the pulmonary resistance, thereby producing immediate bronchial constriction[31], the development of methanol sensor has become essential and urgent, in the present times.

We have tried to study the sensing behaviour of CdSe nano particles towards methanol gas, as less number of CdSe based gas sensors are developed yet. Moreover due to the wide band gap, ZnO based materials are widely used for detecting the toxic and harmful gases because of its superior physicochemical properties. Thereby we have also tried to study the sensing behaviour of CdSe/ZnO Nanoparticles towards methanol gas.

2. Materials and Methods

2.1 Materials

The precursors used in our work were purchased from Merck, India and therefore used directly, as they were of analytical grade. The precursors were sodium sulphite (Na_2SO_3), selenium powder (Se), cadmium acetate [$(Cd(CH_3COO)_2)$], zinc nitrate [$Zn(NO_3)_2$] and acetone. Double distilled water was used during the whole reaction process. Polyvinyl alcohol, PVA was used as the capping agent.

2.2 Synthesis of CdSe nanoparticles

The sample synthesis was carried out using a wet chemical tehnique. At first, CdSe sample, C1 was prepared. At first, in 100 mL deionized water, 1 g sodium sulphite solution was prepared and was stirred magnetically at 65°C for almost two hours. Also a solution of 0.5 g selenium powder in 50 mL distilled water was prepared and stirred at 65°C for almost one hour. These two solutions were then mixed in a beaker and stirred magnetically at 85°C for 7 hours. This resulted in the formation of sodium seleno sulphate solution. This final solution was kept overnight for stabilization, after cooling.

0.4 g cadmium acetate solution and solution of 1 g PVA in 50 mL distilled water were also prepared separately and stirred magnetically at 65°C for about 1.5 hours and 3 hours respectively until clear solutions were obtained. A mixture of 50 mL cadmium acetate solution and 20 mL PVA was stirred at 40°C for about 1.50 hours, until homogeneous. At this stage, ammonia solution was added drop wise to this mixure and the pH value of the solution was made >9.0. At last, 20 mL Ne_2SeSO_3 (sodium seleno

sulphate) solution was poured dropwise, for half an hour to this solution. At this stage, the magnetic stirring rate was 590 rpm and the temperature was maintained at 70^0C. A chocolate brown solution was resulted after 60 minutes of stirring indicating the formation of CdSe nanoparticles.

2.3 Deposition of ZnO shell over the CdSe core

For the synthesis of CdSe/ZnO core/shell nanocomposite, a shell of ZnO was deposited over CdSe core which is named as C1Z1. For this, Zn $(NO_3)_2$ has been used as the precursor. 0.7 M $Zn(NO_3)_2$ solution was prepared in 25 mL de-ionized water and stirred for one hour at 40°C. This solution was then slowly added to 20 mL of previously prepared CdSe solution with pH 11.5, under magnetic stirring. The temperature of reaction was 40°C and the reaction was continued for 30 minutes. A transparent white to milky white transition in the colour of the solution was observed. The shell precursor was 0.7 M and the total reaction time was 210 minutes. The synthesized CdSe and CdSe/ZnO samples are shown in the Fig. 1.

2.4 Characterization methods adopted

The as-synthesized nanoparticles were characterized using a variety of techniques. Using a CuKα (lambda = 1.54A0) radiation-equipped Philips X' Pert powder X-ray diffract meter, the crystalline properties of the samples were examined via X-ray diffraction. A UV-visible spectrophotometer (HITACHI model U-3210) that provides the absorption spectra of all samples over a spectral range of 300 nm to 800 nm was used to study the optical properties. The fluorescence spectra were recorded using a photoluminescence spectrophotometer (Hitachi model F-2500). Using a scanning electron microscope (Model No. Sigma 300), the surface morphology of the samples was examined. Transmission electron microscopy (JEOL2100F model number) is used to study lattice spacing, SAED, and particle distribution.

3 Results and Discussion

The following sections discuss the results using different characterization techniques:

3.1 Mechanism of reaction

The following describes the mechanism of the chemical reaction that takes place during the synthesis of the core nanoparticles[32]

Step 1:

$$Se + Na_2SO_3 \longrightarrow Na_2SeSO_3$$

Step 2:

$$Cd(CH_3COO)_2 \longrightarrow Cd^{2+} + 2CH_3COO^-$$

Step 3:

$$Cd(CH_3COO)_2 + 2NH_4OH\ Cd \longrightarrow (NH_3CH_3COO)_2 + 2H_2O$$

Step 4:

$$Cd(NH_3CH_3COO)_2 + Na_2SeSO_3 + H_2O \longrightarrow CdSe + Na_2SO_4 + 2\ NH_4(CH_3COO)$$

Step 5:

$$CdSeCd^{2+} + \longrightarrow Se^{2-}$$[31]

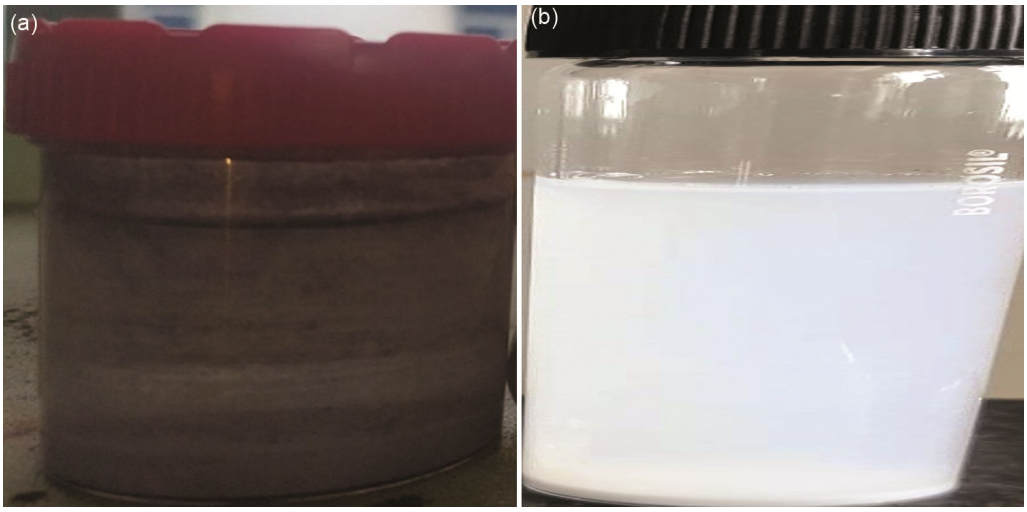

Fig. 1 — (a) CdSe sample, and (b)CdSe/ZnO sample.

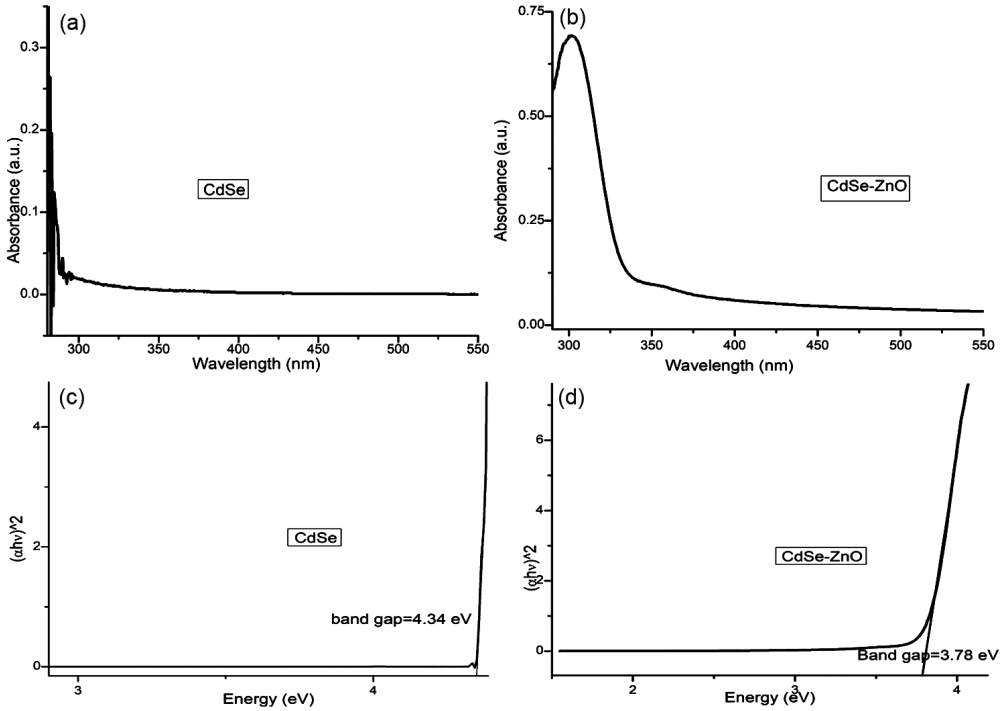

Fig. 2 — (a) Absorption spectra of C1, (b) Absorption spectra of C1Z1, (c) Tauc's plot of C1, and (d) Tauc's plot of C1Z1.

Table 1 — Absorption edge position and values of band gaps for C1 and C1Z1.

Sl. No.	Sample Code	Sample name	Position of Absorption Edge of samples (nm)	Band Gap of Samples (eV)
1	C1	CdSe	292.92	4.34
2	C1Z1	CdSe/ZnO	337.78	3.78

3.2 UV-vis analysis

Figure 2 displays the UV-Vis absorption spectra of the synthesized samples C1 and C1Z1. The CdSe sample's absorption edge was found to be at 292.92 nm, clearly exhibiting a blue shift from its bulk value of 712 nm. The Tauc's relation, which is provided below[33], has been used to estimate the energy band gap value for the sample.

$$\alpha h\nu = (h\nu - E_g)^n \quad \ldots (1)$$

Here, hυ is the energy of incident light, E_g is the material's energy band gap, and α is the absorption coefficient. The type of transition determines the value of n. The values of n for direct and indirect transitions are ½ and 2, respectively. It can be observed that the band gap values are larger than the 1.74 eV band gap value of bulk CdSe, which validates the formation of CdSe nanoparticles. Figures 2(a) and 2(b) show the absorption spectra of the CdSe and CdSe/ZnO samples, respectively, and Figs. 2(c) and 2(d) display the corresponding Tauc's Plots for the samples. Comparing the absorption edge of the core/shell composite sample C1Z1 to that of the CdSe core sample C1, a red shift is observed. This is because the shell that was deposited over the CdSe core caused the nanoparticles' particle size to increase. Consequently, the red-shifting verifies that the shell has been deposited over the core nanoparticles. As a result, in comparison to the core sample, the band gap values of the core/shell composite sample also decrease. The band gap and absorption edge values for both samples are displayed in Table 1.

3.3 Particle size calculation

Using the Brus equation given in (2) below, size of the core nanoparticle has been determined from the UV data**:**

$$R^2 = h^2/8E_x(1/m_e^* + 1/m_h^*) \quad \ldots (2)$$

where, Ex = E – Eg (CdSe). Here, E corresponds to the value of energy band gap obtained using Tauc's Plots and Eg = 1.74 eV corresponds to the energy band gap for bulk CdSe, m_e^* (CdSe) = $0.13m_0$ (m_0 is the mass of free electron),

m_h*(CdSe) = 0.45m_h, and h represents the Planck's constant. The particle size obtained for CdSe Nanoparticles is 2.54 nm while for CdSe-ZnO Nanoparticles is obtained 3.01nm. These values are shown in Table 2.

3.4 Photoluminescence study

One helpful characterization method that offers valuable insights into the optical and photochemical properties of a semiconductor is photoluminescence spectroscopy.

The photoluminescence spectra for C1 and C1Z1 are shown in the Fig. 3 below. The samples are photo-excited at a wavelength of 310 nm. The excitonic emission for core C1 appears at 322.82 nm and for C1Z1 CdSe/ZnO core/shell nanocomposite, the excitonic emission is observed at 324.49 nm. Similar results have been reported by P Gupta *et al.*[34] and I B. Muh'd *et al.*[35]. For C1Z1 there is a shoulder at 373.29 nm. This may be 'impurity' emissions originating from surface states or trap states. The excitonic emission peak in C1Z1 is red shifted compared to the corresponding emission of sample C1. This is due to increase in particle size after ZnO shell is deposited over the core sample. The observed PL spectra are shown in the Fig. 3.

Table 2 — Particle size of the synthesized core and core/shell sample using Brus' equation.

Serial no	Sample code	Sample Name	Particle size (nm)
1	C1	CdSe	2.54
2	C1Z1	CdSe/ZnO	3.01

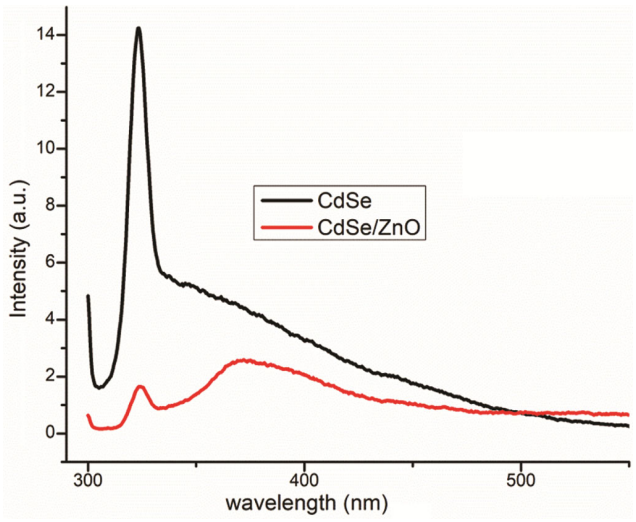

Fig. 3 — Photoluminescence spectra of C1 and C1Z1.

3.5 X-ray diffraction study

XRD patterns of C1 and C1Z1 are shown in Fig. 4. Figure 4 (a) shows the XRD pattern of C1 whereas Fig. 4(b) shows the XRD pattern of sample C1Z1. The diffraction peaks for C1 are at 2θ values of 29.22^0, 30.37^0, 32.09^0, 33.81^0 and 38.61^0 corresponding to the crystal planes (101), (200), (101), (102), and (220) of CdSe respectively. According to JCPDS file No. 01 – 077-2307[36], the presence of reflections from these planes validates that the synthesized material has a hexagonal wurtzite structure. Using the Debye–Scherrer relation, the average crystallite sizes of the synthesised samples were determined to be:

$$D=K\lambda/\beta Cos\theta \quad \ldots (3)$$

In this case, β denotes the diffraction peak's full-width at half maximum (FWHM), K = 0.9, θ is the Bragg's angle, and λ is the wavelength (= 1.54A0) of the CuKα radiation

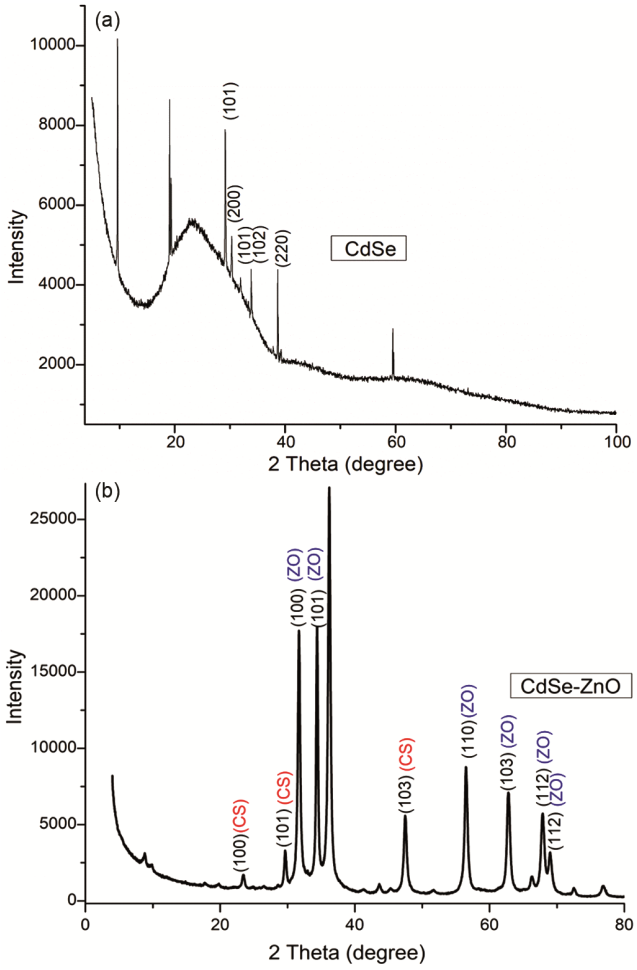

Fig. 4 — (a) XRD pattern of C1, and (b) XRD pattern of C1Z1.

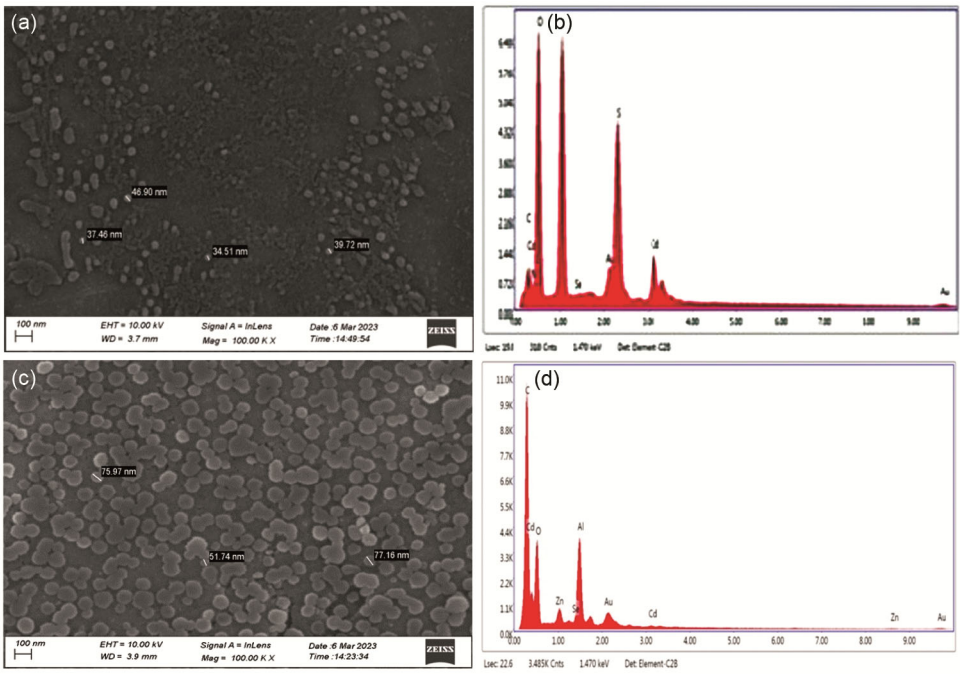

Fig. 5 — (a) SEM image of C1, (b) EDAX pattern of C1, (c) SEM image of C1Z1, and (d) EDAX pattern of C1Z1.

The XRD pattern of C1Z1 is shown in Fig 4(b). The diffraction peaks are consistent with JCPDS file numbers 01-077-2307 for CdSe and 36-1451 for ZnO, respectively. They can be indexed as a mixture of hexagonal wurtzite CdSe and hexagonal wurtzite structure of ZnO[37]. The peaks corresponding to ZnO occur at 31.14°, 34.88°, 56.5°, 63.78, 68.31°, and 69.02° respectively. Using equation (3) the average crystallite sizes for the CdSe/ZnO samples are also calculated. It is found to be 23.81 nm for C1and 31.90 nm for C1Z1respectively. It is found that the average crystallite size of C1Z1 sample is greater than that of core C1 sample. This confirms the deposition of the shell over the core sample.

3.6 SEM and EDAX analysis

The SEM micrograph of the sample images of C1 and C1Z1 are shown in Fig 5 (a-c) and the corresponding EDAX images are shown in Fig. 5 (b-d) respectively. The particles are found to be a most spherical in shape. The particle sizes are in the range 30-50 nm for C1 nanoparticles and 50-70 nm for C1Z1 nanocomposite. Agglomeration of the particles to a certain extent can be observed in the images. The EDAX image confirms the presence of elements Cd and Se in the sample.

The EDAX image also reveals the presence of other elements, such as Ca, O, Na, Mg, Au, Si, and so forth. The glass slide that served as a substrate for the prepared CdSe sample's deposition may have produced the Si and O. The remaining elements might be present because of the coating on the semiconductor nanomaterial that was used for the analysis. Coating is essential in SEM analysis to facilitate or enhance sample imaging. It lessens thermal damage and enhances the secondary electron signal, both of which are necessary for the SEM's topographic analysis.

3.7 TEM/HRTEM

The TEM/HRTEM images of sample C1 and C1Z1 are shown in Figs 6 and 7. From the images the CdSe nanoparticles are observed to be almost spherical in shape. The particle sizes are having sizes in the range 5-20 nm. The lattice spacing for CdSe nanoparticles, C1 was found to be 0.42 nm. The particle sizes of the CdSe/ZnO sample, C1Z1 were found to be in a range of 40-80 nm which is larger in comparison to the core C1 nanoparticles. Concentric rings in the SAED patterns for both the CdSe(C1) and CdSe/ZnO (C1Z1) sample show the formation of good crystalline structure for both CdSe nanoparticles and CdSe/ZnO nano composite. The particle size distribution histograms shows that for the CdSe nanoparticles, C1, most of the nanoparticles are in a range of 70-80 nm. On the other hand for the CdSe/ZnO nanocomposite, C1Z1, most of the particles are found to in a range of

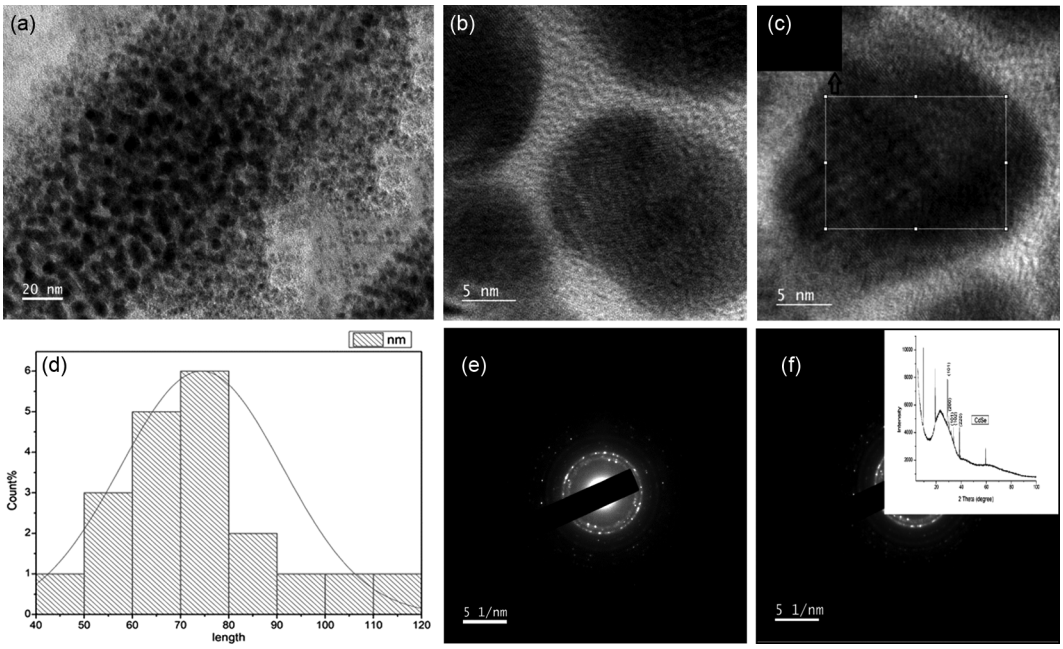

Fig. 6 — (a) TEM, (b) HRTEM, (c) Lattice spacing Images, (d) Histogram showing particle size distribution, (e) SAED pattern of CdSe(C1) nanoparticles, and (f) Miller indices of SAED pattern.

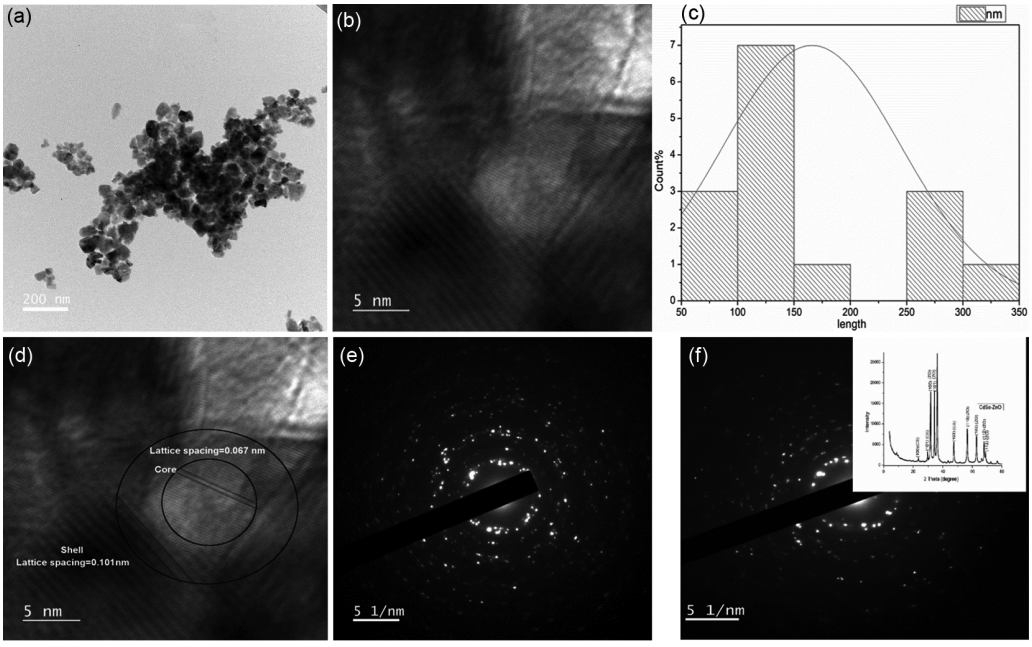

Fig. 7 — (a) TEM, (b) HRTEM image, (c) Histogram showing particle size distribution (d) Lattice spacing image, (e) SAED pattern of CdSe-ZnO (C1Z1) Nanoparticles, and (f) Miller indices of SAED pattern

100-150 nm. The lattice spacing of ZnO shell material over CdSe core material was found to be 0.101 nm while for core CdSe Nanoparticles it was found to be 0.067 nm.

3.8 Gas sensing studies

Gas sensing ability of a material depends upon various parameters. The parameters include surfacedefects, surface morphology, film thickness, speed of the chemical reaction on the surface of the material, particle size etc. The resistance of a particular material may change after diffusion of the molecules of gases on the material's surface. This change in resistance can be expressed in terms of sensitivity (S %) of the sensor[38]. In this present work we have studied the

selectivity of CdSe and CdSe-ZnO samples towards various gases such as ammonia (NH_3), ethanol (C_2H_5OH), acetone (C_2H_6OR), formaldehyde (CH_2O) and methanol (CH_3OH) respectively. Our sensor was found to be more selective towards methanol gas and so the sensing studies have been performed using methanol.

3.9 Selectivity study

The response of a sensor for different gases viz. ammonia, ethanol, acetone, LPG, sulphur dioxide, carbon dioxide etc. in presence of other gases, is termed as selectivity[39]. It is measured in terms of selectivity coefficient which is defined as

$$S = S_A / S_B \quad \ldots (4)$$

Where, S_A and S_B are the resistances of the sensor in air and in the presence of the inserted gas respectively.

In this work, we have carried out experiments for measurements of sensitivity, response and recovery time of the synthesized CdSe and CdSe/ZnO core/shell nanocomposites. From the selectivity graph shown in Fig. 8 of CdSe, C1, nanoparticles, it is observed that, when different gases such as ethanol, methanol, ammonia, formaldehyde and acetone are inserted into the reaction chamber, the resistance of the CdSe (C1) sample decreases with respect to time. We observed that the change in resistance of C1, in presence of methanol gas is large in comparison to the other inserted gases and decreases smoothly until it attains a steady state. For ammonia and acetone the resistance of the sample remains almost unchanged. When ethanol and formal dehyde gas are inserted into the chamber, the resistance of C1decreases as shown in Fig. 8. It is observed from the figure that, the decrease in resistance of the sensor, in presence of methanol gas is quite large as compared to formaldehyde and ethanol gases. Hence from this study we can conclude that, sample C1 is more selective towards methanol gas. Thus the sensitivity studies of the sensor have been carried out for methanol gas as detailed in the next sections.

3.10 Gas sensitivity study

To investigate the sensing properties of CdSe and CdSe-ZnO samples towards methanol gas we have measured the change in resistance of the samples in comparison to the open air resistance upon intake of gas. The sensitivity[40] may be defined by Eq. (5)

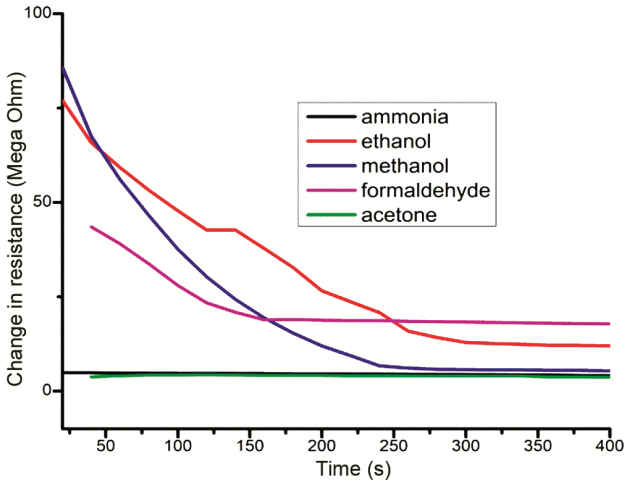

Fig. 8 — Selectivity graph of C1.

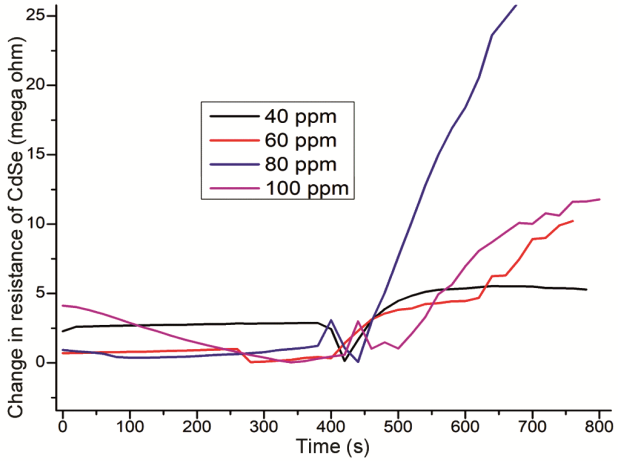

Fig. 9 — Resistance variation versus time graph of C1.

$$S = R_g\text{-}R_a / R_a \quad \ldots (5)$$

Where R_g is the sensor resistance in presence of target gas and R_a is the sensor resistance in air. Figures 9 and 10, show the response of CdSe, C1 and CdSe/ZnO, C1Z1, core/shell nano composites towards methanol gas for both Gas ON(0 to 400 secs) and Gas OFF(400 to 800 secs) conditions for different gas concentrations (40-120) ppm at room temperature. For the CdSe nanoparticles, in GAS ON condition, we observed that there is no significant change sensor resistance (difference between open air resistance and resistance in presence of methanol) in the GAS ON condition, except a decrease in the value for 100 ppm. However, in the GAS OFF condition, the change in resistivity and hence the sensitivity (shown in Fig. 11) increases with increase in time. The open air resistance of CdSe nanoparticles was measured at first and was found to be 5.01 MΩ. This was followed by

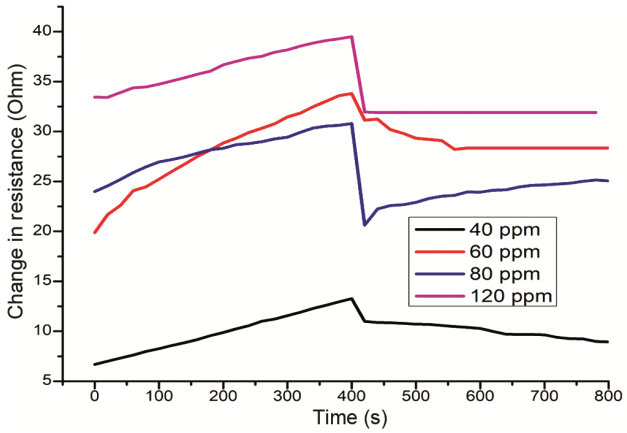

Fig. 10 — Resistance variation versus time graph of C1Z1.

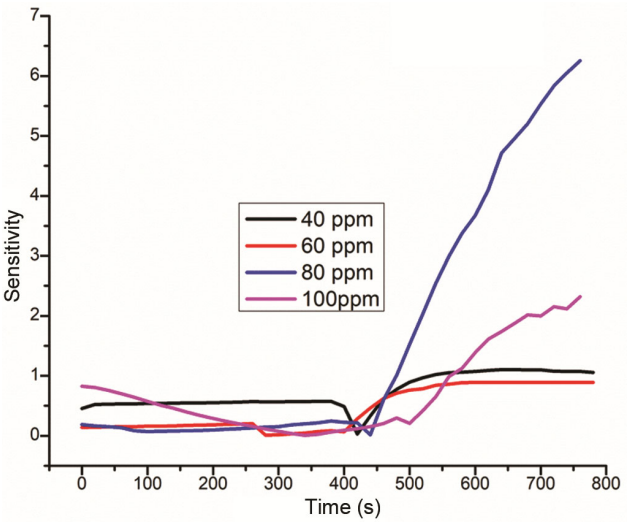

Fig. 11 — Sensitivity graph of C1.

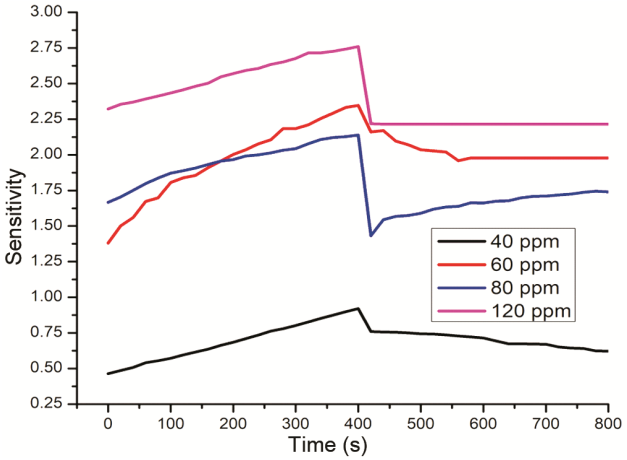

Fig. 12 — Sensitivity graph of C1Z1.

measurement of sensor resistance in the presence of methanol with the increase in time. But for the CdSe/ZnO, C1Z1, core/shell nanocomposite, for GAS ON condition, the change in resistance was found to increase with the increase in time and underwent a sharp decrease immediately when the gas is switched off and then became more or less steady, in the GAS OFF condition. Moreover, it was observed that as the gas concentration increased from 40 to 120 ppm, the value of change in resistance of the sensor increases. The open air resistance for the CdSe/ZnO nanocomposite was found to be 14.4 KΩ. Thus, for the CdSe/ZnO core/shell sample the sensitivity increases in the GAS ON condition and decreases in the GAS OFF condition as shown in Fig. 12. We found that, as the gas concentration was increased the sensitivity of the sensor also increased.

3.11 Response and recovery plots of CdSe nanoparticles and CdSe/ZnOnanocomposite

The time required by a sensor to reach the particular percentage level (usually 90%), of the saturation value upon exposure to a target gas is termed as the sensor's response time[41]. Whereas, the time required by a sensor to return to its 10% of the original baseline when the target gas is removed from the sample, is termed as the recovery time[41].

The response and recovery plots of CdSe, C1 and CdSe/ZnO, C1Z1 samples, towards methanol gas are shown in Fig 13. From the response curve of C1 is shown in Fig. 13 (a). It can be seen that, the response time increases from 20 sec to 250 sec with increase in concentration from 40 ppm to 100 ppm. From the response curve of C1Z1, given in Fig. 13 (c), it is observed that, the response time increases from 18 sec to 300 sec with increase in gas concentration from 40 to 100 ppm. From the recovery curve of C1 and C1Z1, shown in Figs. 13 (b) and 13 (d) respectively, it is observed that the recovery time at first decreases and then increases with increase in gas concentration.

3.12 Sensitivity of the sensor towards methanol in presence of ethanol and vice versa

As the selectivity graphs C1 sample shown in Fig. 8 shows some response towards ethanol gas (although less in comparison to methanol), we attempted to study the response of the sensor C1Z1 towards ethanol gas, in presence of methanol gas and vice versa. The graphs are shown in Figs. 14 (a) and 14 (b), respectively. Figure 14(a) depicts the resistance of the C1Z1 towards methanol gas (40 ppm). It is found that the sensor resistance at first

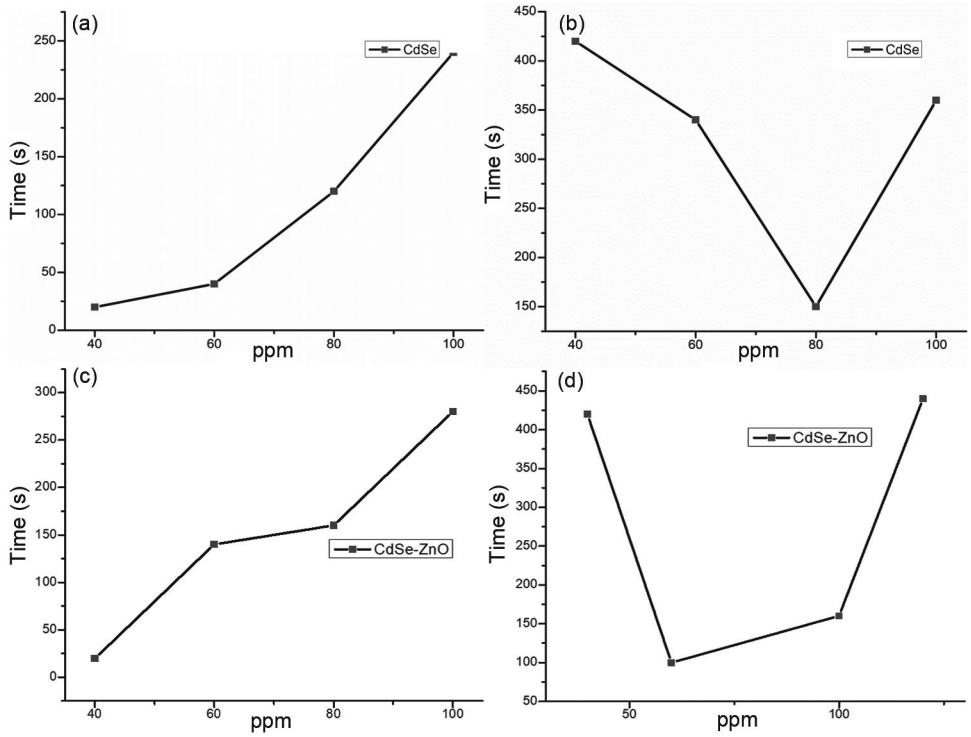

Fig. 13 — (a) Variation of response time of CdSe C1, (b) Variation of recovery time of CdSe C1, (c) Variation of response time of CdSe/ ZnO C1Z1 and (d)Variation of recovery time of CdSe/ ZnO C1Z1.

decreases in the GAS ON condition and becomes stable in the GAS OFF condition. With methanol gas being present within the reaction chamber, we have inserted 40 ppm of ethanol gas into it, and it is found that, the sensor resistance increases slightly at the beginning and then remains unchanged in the GAS ON condition. However, when gas is switched off, the resistance starts increasing in the GAS OFF condition. In a similar manner, as shown in Fig. 14 (b), the response of the sensor towards 40 ppm ethanol gas was at first measured, which did not show any significant change in resistance. However, when methanol gas was inserted into the chamber, with ethanol already present in it, a significant change in resistance is observed in both GAS ON and GAS OFF conditions. This confirms that, the C1Z1 sensor is selectively sensitive towards methanol gas only.

3.13 Gas sensing mechanism

From the results obtained for methanol sensing of CdSe, C1 and CdSe/ZnO, C1Z1nanocomposite, it can be understood that, the CdSe/ZnO nanoparticles are acting as better sensor for methanol gas. This is due to the role played by the ZnO shell layer, over the CdSe core. The function of the ZnO layer can be understood from the surface charge model[42].At first when the CdSe nanoparticles are exposed to air, its surface is surrounded by various chemical species and oxygen molecules get adsorbed on the semiconductor surface[34]. These molecules of oxygen traps electrons from the conduction band of CdSe, due to which absorbed oxygen species are created as given below[42]:

$$O_2\,(g) \longrightarrow O_2\,(ads)$$

$$O_2\,(ads) + e^- \longrightarrow O^{2-}$$

This results in the formation of a depletion layer on the surface of CdSe. As a result, the resistance of the semiconductor changes. When methanol gas is inserted into the reaction chamber, the ions of oxygen on the surface of the semiconductor, reacts with the methanol molecules, thereby releasing the trapped electrons back to the conduction band of CdSe.

The reaction which occurs among the methanol molecules and the oxygen ions are shown below:

$$CH_3CH_2(ads) + O^-(ads) \longrightarrow C_2H_4O + H_2O + e^-$$

$$CH_3CH_2OH + O^{2-}(ads) \longrightarrow C_2H_4O + H_2O + 2e^-$$

As a result, the resistance of the CdSe semiconductor will change.

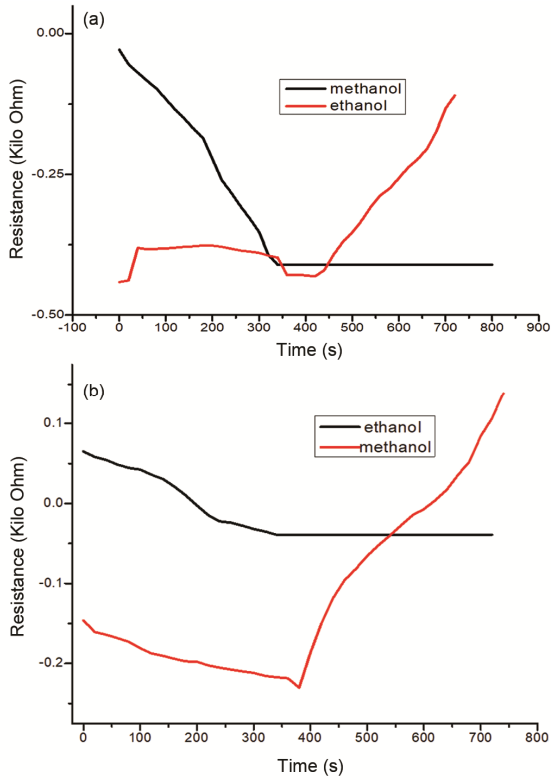

Fig. 14 — (a) Plot showing values of resistance with time (ethanol in presence of methanol gas) for C1Z1, and (b) Plot showing values of resistance with time (methanol in presence of ethanol gas) for C1Z1.

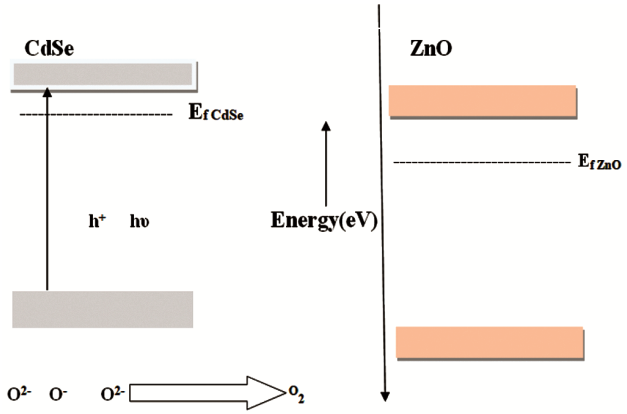

Fig. 15 — Schematic model of CdSe/ZnO sensors when exposed to methanol.

However, for the CdSe/ZnO, nanocomposite, an additional depletion layer will be created, due to the presence of ZnO. This will affect the transport of charges within the structure[30]. It is known that, the Fermi Level of CdSe is at higher energy, than that of ZnO. As such the electrons in CdSe will get transferred to ZnO, which in turn will result in the creation of the additional depletion layer at the interface between CdSe and CdSe/ZnO. Thus when the hetero structure, is exposed to methanol gas, the electrons will be released quite easily from the surface, back to the conduction band of ZnO, resulting in a change in the sensor resistance. In all, we can say that CdSe/ZnO nanostructure will possess more active sites for oxygen adsorption, which will make it a better sensor for methanol, compared to single CdSe. A schematic model depicting the reaction mechanism is shown in Fig 15.

3.14 Limit of detection

The limit of detection of CdSe/ZnO, C1Z1 Nano composite towards methanol gas is calculated using equation given below[43]

$$LOD=3.0*\sigma/S$$

where S is the calibration curve's slope, σ is the relative standard deviation, and 73.00 ppm is the determined limit of detection.

4 Conclusion

It can be concluded that, hexagonal CdSe and CdSe/ZnO core/shell nanocomposite have been successfully synthesized in this work. Various characterization techniques, including UV-visible spectroscopy, photoluminescence spectroscopy, XRD, SEM, EDAX, and TEM, have confirmed the formation of both core CdSe nanoparticles and core/shell CdSe/ZnO nanocomposite. When compared to the bulk value of CdSe, the absorption edges obtained from UV-visible spectroscopy results of the CdSe and CdSe/ZnO samples exhibit a blue shift.

This confirms the formation of nanostructures of both CdSe and CdSe/ZnO. The CdSe and CdSe-ZnO samples show more selective behaviors in sensing methanol gas compared to ethanol, acetone, formaldehyde and ammonia. From the sensitivity study for both CdSe and CdSe/ZnO core/shell nanoparticles it can be reported that the ZnO based sensor is better sensor as compared to the bare CdSe sensor in detecting methanol gas.

Acknowledgement

The authors sincerely acknowledge the Department of Chemistry, Gauhati University for their help in availing the SEM and EDAX facilities, the Department of Instrumentation and USIC, Gauhati University for XRD facility and CIF, IIT Guwahati for providing the TEM/HRTEM analysis of the samples. The first author

(Pallabi Boro) also acknowledges CSIR, New Delhi for the financial support under JRF scheme [File no-09/059(0066)/2018-EMR-I, date: 22/02/2019].

References

1 Abideen Z U, Kim J H , Lee J H, Kim J Y, Mirzaei A, Kim H W & Kim S S, *J Korean Ceram Soc*, 54 (2017) 366.
2 Wang C, Yin L, Zhang L & Gao R, *Sensors*, 10(2010) 2088.
3 Sowmya B, John A & Panda P K, *Sensors International*, 2(2021) 100085.
4 https://www.sciencedirect.com/topics/engineering/gas-sensor
5 Sun Y F, Liu S B, Meng F L, Liu J Y, Jin Z, Kong L T& Liu J H*, Sensors,* 12 (2012) 2610.
6 Hegazy M A, Abd El-Hameed A M, NRIAG J, *Astron. Geophys*, 3 (2014) 82.
7 Shahi A K , Pandey B K , Singh B P &Gopal R, *Adv Nat Sci, Nanosci. Nanotechnol*, 7, 2043 (2016).
8 Terna A D, Elemik E E, Mbonu J I, Osafile O E, Ezeani R O, *Mater SciEng,* B 272 (2021) 115363.
9 Chaudhari K B, Gosavi N M, Deshpande N G & Gosavi S R, *J SciAdv Matter Dev*, 1 (2016) 476.
10 Mansournia M, Rafizadeh S, H Mashkani S M H & Motaghedifard M H, *Mater. Sci. Eng. C*, 65 (2016) 303.
11 Rakgalakane B P, Moloto M J, *J. Nanomater*, 514205 (2011) 1
12 Chizhov A S, Rumyantseva M N, Vasiliev R B, Filatova D G, Drozdov K A, Krylov I V, Abakumov A M & Gaskov A M, *Sensor Actuat B-Chem*, 205 (2014) 305.
13 Shan G, Kong X, Wang X & Liu Y, *Surf. Sci,* 582 (2005) 61
14 Suo B, Su X, Wu J, Chen D, Wang A, Guo Z, *Mater Chem Phys*, 119 (2010) 237.
15 Nikam P R, Baviskar P K, Majumder S, Sali JV, *Sankapal B R J Interface Sci*, 524 (2018)148.
16 WangL, Han J, Wu Y, Zhang Y, Zhang Q, Tan X, Yang Y, Li W, Bu Y & Ao J-P, *Chem Eng J*, 368 (2019) 710.
17 Li Z, Jin D & Wang Z, *Appl Surf Sci.*, 529(2020) 1.
18 Nazemi H, Joseph A, Park J & Emadi A, *Sensors*, 11 (2019).
19 Chavali M S & Nikolova M P, *SN Appli. Sci*, 1 (2019) 607.
20 Terna A D, Elemike E E, Mbonu J I, Osafile O E & Ezeani R O, *Mater Sci Eng B,* 272 (2021).
21 Kim H J, Lee J H, *Sens. Actuators B Chem,* 192(2014) 607.
22 Johnson Matthey, *Technol. Rev*, 61(2017)172.
23 [Editor Osterloh J D, *Environmental Medicine: Integrating a Missing Element into Medical Education* (National Academic Press, Washington D C , 1995)]
24 Zhang J, Qin Z, Zeng D & Xie C, *Phys Chem Chem Phys*, 19(2017) 6313.
25 Ando M, Kamimura T, Uegaki K, Biju V, Damasco Ty J T & Shigeri Y, *SensActuators B: Chem*, 246(2017) 1074.
26 Broek J V, Bischof D, Derron N, Abegg S, Gerber P A, Giinter A T & Pratsinis S E, *Anal Chem* , 93 (2021) 1170.
27 Chizhov A S, Rumyantseva M N, Vasiliev R B, Filatova D G, Drozdov K A, Krylov I V, Abakumov A M & Gaskov A M, *Sens Actuators B Chem*, 205 (2014) 305.
28 Abdullah M M, Faisal M, Ahmed J, Harraz FA, Jalalah M, Alsarei S A, *J Electro chem Soc,* 168 (2021).
29 Wu B, Lin Z, Sheng M, Hou S & Xu J, *Appl Surf Sci*, 360 (2016) 652.
30 Broek J V D, Abegg S, Pratsinis S E & Güntner A T, *Nature. com*, 10 (2019) 1.
31 Rong Q, Zhang Y, Wamg C, Zhu Z, Zhang J & Liu Q, Sci. Rep., 7 (2017) 1.
32 Devi S R, Sing R K L, *Nath S S, Chalcogenide Lett*., 10, 4(2013) 151.
33 Surana K, Singh P K, Rhee H-W & Bhattacharya B, *J. Ind Eng Chem*, 20(2014) 3913.
34 Gupta P & Ramrakhiani M, *The Open Nanosci*. J, 3 (2009) 15.
35 Muh'd I B, Talib Z A, Zainal Z & Liew J Y C, *J Nano*, 2017, 2083819 (2017).
36 Gupta D K, Verma M, Sharma K B & Saxena N S, *Indian J Pure App. Phy*, 55 113(2017).
37 JCPDS, Joint Committee for Powder Diffraction Standards, Power Diffraction File for Inorganic Materials, 1979.
38 Gao X, Zhang T, *Sens Actuators B Chem*, 277 (2018) 604.
39 [www.sciencedirect.com/topics/engineering/gas-sensor (24April 2024)].
40 Kumar R, Dossary O A, Kumar G & Umar A, *Nano-Micro Lett*, 7 (2015) 97.
41 Mirzaei A, Lee J-H, Majhi S M, Weber M, Bechelany M, Kim H W & Kim S S, *J Appl Phys*,126 (2019).
42 Hongsitha N, Wongrat E, Kerdcharoen T, *Choopun S,Sens Actuators B*, 144 (2010) 67.
43 Das M, Sarkar D, One, Ceram. Int. 43 (2017) 11123.